

# On the role of evanescent modes and group index tapering in slow light photonic crystal waveguide coupling efficiency

Amir Hosseini,<sup>1,a)</sup> Xiaochuan Xu,<sup>1</sup> David N. Kwong,<sup>1</sup> Harish Subbaraman,<sup>2</sup> Wei Jiang,<sup>3</sup> and Ray T. Chen<sup>1,b)</sup>

<sup>1</sup>Department of Electrical and Computer Engineering, The University of Texas at Austin, Austin, Texas 78712, USA

<sup>2</sup>Omega Optics, Inc., 10306 Sausalito Dr., Austin, Texas 78759, USA

<sup>3</sup>Department of Electrical and Computer Engineering, Rutgers University, Piscataway, New Jersey 08854, USA

(Received 29 November 2010; accepted 5 January 2011; published online 21 January 2011)

We investigate effects of different mechanisms on coupling efficiency between strip waveguides and the slow light mode in photonic crystal waveguides (PCWs). Both numerical simulations and experimental results show that group index ( $n_g$ ) tapering improves strip-PCW butt-coupling efficiency when compared to a direct coupling between a strip waveguide and a high- $n_g$  PCW. However, coupling efficiency is even higher when an intermediate low- $n_g$  PCW is used to couple from a strip waveguide to a high- $n_g$  PCW without an  $n_g$  tapering. Our results suggest that the role of evanescent mode is more dominant in efficient coupling between two PCWs with large  $n_g$  mismatch. © 2011 American Institute of Physics. [doi:10.1063/1.3548557]

Slow light in photonic crystal waveguides (PCWs) has been extensively studied for potential on-chip applications such as optical buffers and enhanced nonlinearity due to increased light-matter interaction.<sup>1</sup> The enhanced light-matter interaction provided by the slow light operation can be exploited, resulting in ultracompact on-chip photonic devices.<sup>2</sup> Recently, over 40 GHz modulation speed using the slow light mode in slot photonic crystals refilled with electro-optic polymer has been demonstrated.<sup>3</sup> However, the issue of large insertion losses due to strong impedance mismatch between strip waveguides and the PCW slow light mode needs to be addressed before integration of several slow light PCW devices is feasible.

Different approaches were proposed to enhance the coupling efficiency between strip waveguides and the PCW slow light mode. Optimization of the PCW termination at its interface with the access waveguides was presented in Ref. 4. However, this approach does not enhance light coupling into the modes near the band-edge, where slow light based devices and other band-edge devices (such as in Ref. 5) operate. Demonstration of enhanced coupling by inserting a low group index ( $n_g$ ) PCW between the strip waveguide and the slow light PCW (high  $n_g$ ) was first presented in Ref. 6, where over 100  $\mu\text{m}$  of low- $n_g$  PCW was used for efficient light coupling. Adiabatic tapering of the group index for efficient coupling was suggested<sup>7,8</sup> and experimentally demonstrated.<sup>9</sup> In these types of structures, a PCW taper is used as the coupler with its group index band engineered to change from that of the high- $n_g$  ( $>20$ ) PCW to a much smaller value ( $n_g=4-8$ ) over several (4-16) periods, which gives a relatively short coupler. The operating principle relies simply on reducing the light reflectance ( $R$ ) at discontinuities based on the effective medium approximation  $R=(n_{g1}-n_{g2})^2/(n_{g1}+n_{g2})^2$ , where  $n_{g1}$  and  $n_{g2}$  are group indices of

the two PCWs at either side of the discontinuity. However, using this relation in the case of hexagonal lattices (with air holes), which is the most common on-chip structure for PCWs, leads to significant underestimation of the coupling efficiency values reported before [e.g.,  $n_{g1}=5$ ,  $n_{g2}=100$ ,  $T=1-R=80\%$  (Ref. 10)]. It has been argued that the high transmission is due to the excitation of an evanescent mode on the high- $n_g$  side of the interface.<sup>10,11</sup> The evanescent mode has amplitude comparable to that of the fundamental propagating mode, and its phase is such that it results in a small total field at the interface with the low- $n_g$  PCW to satisfy the boundary conditions. Away from the interface, however, the evanescent mode decays and the total field amplitude increases to its maximum. Note that the final field amplitude in the high- $n_g$  PCW is much larger than that in the low- $n_g$  PCW due to the slowdown effect. In this letter, we compare the effect of evanescent modes and group index tapering on the total coupling efficiency from a strip waveguide to a high- $n_g$  PCW. We numerically investigate the effect of PCW taper [see Fig. 1(a)] with different lengths and tapering profiles, including a step profile. We also present experimental results of fabricated PCWs on a silicon-on-insulator (SOI) substrate.

A schematic of a strip waveguide to a high- $n_g$  PCW structure with an intermediate low- $n_g$  PCW coupling structure is shown in Fig. 1(a). The high- $n_g$  PCW is a W1.0 PCW ( $d_0=a\sqrt{3}$ ), where  $a=395$  nm is the lattice constant. Hole radii for both the PCWs are the same,  $r=0.26a$ . The width of the line defect in the PCW taper changes from  $d_{i1}$  at the interface with the high- $n_g$  PCW to  $d_{iN}$ , which is set to be  $a(\sqrt{3}+0.2)$  at the interface with the strip waveguide.  $N$  is the number of periods in the PCW taper. SOI with a silicon device layer thickness of 230 nm is assumed. In the case of a step taper, the line defect width is constant throughout the taper; also  $d_{i1}=d_{i2}\cdots=d_{iN}$ . In the case of adiabatic tapers,  $d_{ii}$  values assume either a linear or a parabolic profile from  $d_0$  to  $d_{iN}$ . In the case of split tapers,  $d_{i1}=\cdots=d_{i,N/2}=a(\sqrt{3}+0.1)$  and  $d_{i,N/2+1}=\cdots=d_{iN}=a(\sqrt{3}+0.2)$ . Note that the step taper is the same as the hetero-group-velocity PCWs investigated in

<sup>a)</sup> Author to whom correspondence should be addressed. Electronic mail: ah@amiryv.com.

<sup>b)</sup> Electronic mail: raychen@uts.cc.utexas.edu.

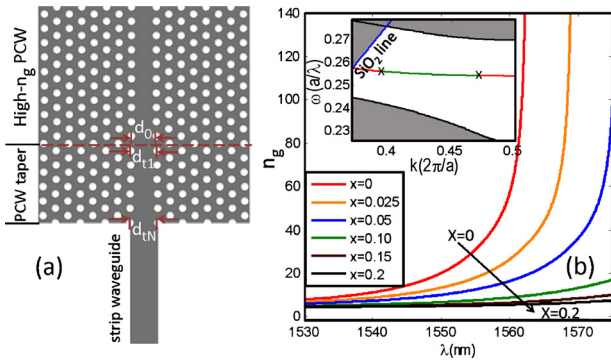


FIG. 1. (Color online) (a) A schematic of the strip waveguide to high- $n_g$  photonic crystal waveguide coupling structure. The PCW on the right side of the interface is assumed to support high- $n_g$  propagation at the wavelength of operation. (b) Group index vs wavelength for infinitely long PCW with different defect line widths,  $d_0 = a(\sqrt{3} + x)$ . The inset shows band structure for W1 PCW,  $r = 0.26a$ , slab thickness = 230 nm,  $n(\text{SiO}_2) = 1.45$ , and  $n(\text{Si}) = 3.47$ . The highlighted (green) section is the bandwidth over which  $20 < n_g < 100$ .

Ref. 6, with the difference that we consider much shorter low- $n_g$  PCW tapers ( $N \leq 16$ , PCW taper length  $< 7 \mu\text{m}$ ).

In order to calculate the group index, we simulate the PCW band structure using three-dimensional (3D) plane wave expansion method. Figure 1(b) inset shows the band structure for a W1 PCW. Figure 1(b) shows variations of  $n_g$  as a function of wavelength for PCWs with various line defect widths. A gradual increase in the line defect width can be used for adiabatic tapering for the group index based on the same technique used in Refs. 8 and 9. Note that further widening the line defect width [more than  $a(\sqrt{3} + 0.2)$ ] does not significantly reduce the group index in the bandwidth of interest ( $20 < n_g < 100$ ).

We use 3D finite difference time domain (FDTD) simulations to calculate the coupling efficiency. In order to isolate the effect of the PCW taper from the Fabry–Perot oscillations due to reflection at the input and output ports, we only simulate one port (one strip waveguide-PCW taper-high- $n_g$  PCW) as shown in Fig. 1(a). In the FDTD simulations, 12 periods of the high- $n_g$  PCW are used. We simulate the coupling transmission for step, linear, parabolic, and split tapers for  $N = 4, 8$ , and 16, as shown in Fig. 2. We observe that for any number of periods, the step taper results in highest transmission almost throughout the slow light region. As the number of periods in the taper increases or as the group index increases, all the taper types result in similar performance. Interestingly, the linear taper and the step taper show similar behavior in the slow light region for all  $N$  values. For  $N = 16$ , when  $n_g > 80$ , both linear and split tapers show a slightly better performance ( $\sim$ with 5%) compared to the step taper. For  $N = 16$ , very close to the band-edge ( $\lambda = 1562.5 \text{ nm}$ ), the parabolic taper outperforms the step taper.

It has been known that backscattering loss in PCWs increases as  $n_g$ .<sup>12</sup> Furthermore, both adiabatically increasing group index in a chirped PCW on a SOI substrate<sup>13</sup> and the transmission spectrum of GaAs PCW membranes<sup>14</sup> have shown that the disorder-induced scattering completely disrupt transmission for  $n_g > 30$ . Therefore, for PCW based slow light devices, in the range of power-law governed transmission, the step taper outperforms the adiabatically and split tapered ones. From the 3D FDTD simulation results we found that step tapering for a small number for periods in the

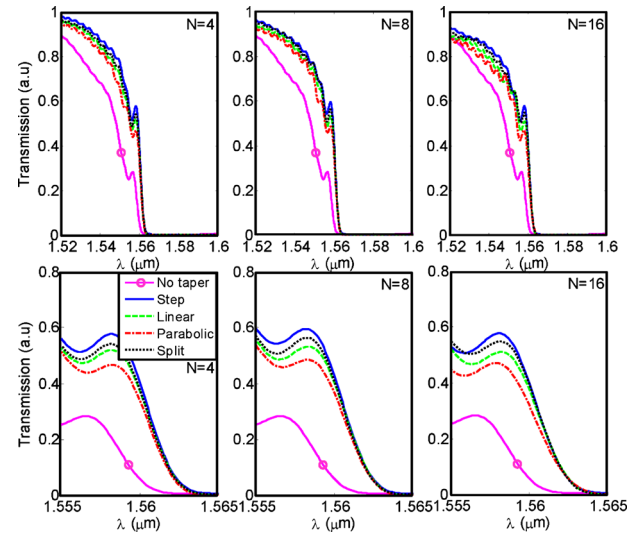


FIG. 2. (Color online) 3D FDTD simulation results for direct coupling of strip waveguide and PCW slab waveguide (no taper) and coupling through PCW tapers, with step, linear, parabolic, and split profiles, for  $N = 4, 8$ , and 16. The lower row graphs were zoomed at the band-edge region.

taper ( $N < 8$ ) has the highest coupling efficiency. The adiabatic tapers only outperform the step taper at  $n_g$  values not supported by the current state of art fabrication technology, and only at longer tapers, which are not desirable in case of compact slow light PCW based devices, which are typically  $\sim 10 \mu\text{m}$  long.<sup>3,5</sup>

Since group index tapering is not present in the step taper, the only explanation for high coupling efficiency between highly group index mismatched PCWs is provided by the existence of evanescent modes at the interface, which helps satisfy the boundary conditions without the need for high reflection.<sup>11</sup> So, we can conclude that the effect of the evanescent mode in coupling between low- $n_g$  and high- $n_g$  PCWs is more dominant than the effect of the group index tapering for practical compact devices. Note that the possibility of reactive energy storage through the evanescent modes at the low- $n_g$  PCW and high- $n_g$  PCW interface is provided by the dramatic difference between the fundamental index guided and gap guided mode field profiles similar to the conditions of supercoupling.<sup>15</sup>

In order to confirm the above claim, we fabricated PCWs on SOI (SOITEC) with a 250 nm top silicon layer and a 3  $\mu\text{m}$  buried oxide layer. A 50 nm oxide layer was thermally grown as an etching mask, consuming 20 nm silicon. The length of the high- $n_g$  PCW section is 100  $\mu\text{m}$  in order to suppress the Fabry–Perot effect on the transmission. The pattern was transferred to the SOI through electron beam lithography system, followed by reactive ion etching. Scanning electron microscope (SEM) pictures of fabricated devices are shown in Fig. 3.

The photonic crystal waveguide was tested on a Newport six-axis autoaligning station. The light from a broadband amplified spontaneous emission source, covering 1520–1620 nm, was TE-polarized with an extinction ratio of over 20 dB and was butt coupled into/out through a polarization maintaining lensed fiber with a mode diameter of 2.5  $\mu\text{m}$ . The transmitted light was analyzed by an optical spectrum analyzer with 0.05 nm resolution. Figure 4 shows the transmission spectra of direct coupling between strip waveguide and PCW, and also coupling through step and linear PCW tapers

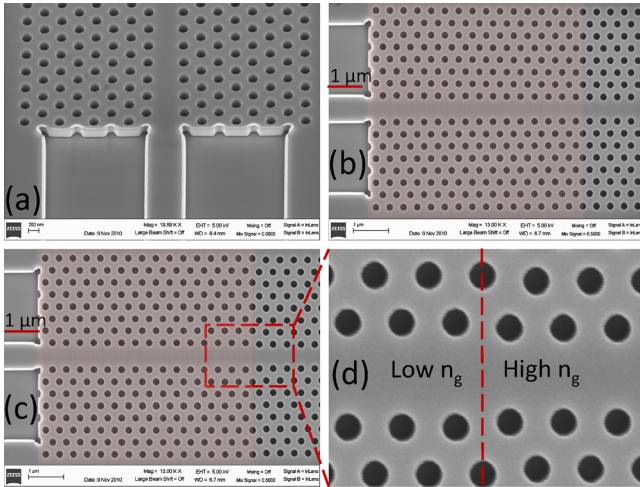


FIG. 3. (Color online) SEM picture of fabrication PCW butt coupled to strip waveguides: (a) a tilted view showing the silicon slab PCW, (b) 16-period linear taper, (c) 16-period step taper, and (d) interface of step taper with high- $n_g$  PCW.

with 8 and 16 periods. The oscillation amplitude for the direct coupling is 6 dB (full swing), while it is about 3 dB for coupling with either step or linear tapers,  $N=8$  and 16. The transmission spectra are blueshifted by about 20 nm, which is due to 15 nm expansion in the hole diameter. Similar to the 3D FDTD results, the step tapers slightly outperform the

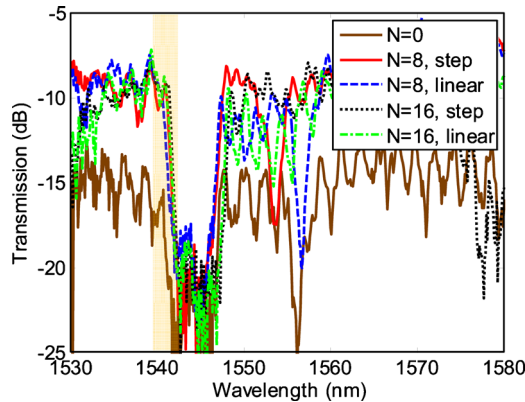


FIG. 4. (Color online) Measurement results: transmission vs wavelength for direct coupling of strip waveguide and PC slab waveguide (no taper) and coupling through PCW tapers, with step and linear profiles, for  $N=8$  and 16. The near band-edge wavelength (slow light region is highlighted).

linear tapers in both  $N=8$  and 16 cases. Also, as  $N$  increases, performances of the step and linear tapers converge together.

In summary, by comparing the effect of different PCW taper profiles on transmission in the slow light region, we investigated whether group index tapering or the existence of evanescent modes at the boundary of a low- $n_g$  and a high- $n_g$  PCW has a dominant role in enhancing light coupling between strip waveguide and a PCW operating in the slow light region. Numerical analysis and experimental measurements showed that the use of short low- $n_g$  PCW as an intermediate coupler, in which group index tapering is absent, is advantageous over adiabatically tapered PCW coupler. Our results also indicate that for an efficient coupling, a low- $n_g$  PCW coupler much shorter (compared to over hundreds of microns of low- $n_g$  PCW coupler in Ref. 6) than previously demonstrated is sufficient.

This research was supported by the AFOSR Multi Disciplinary University Research Initiative (MURI) under Grant No. FA9550-08-1-0394 and AFOSR Small Business Technology Transfer (STTR) under Grant No. FA9550-11-C-0014.

- <sup>1</sup>Y. A. Vlasov, M. O'Boyle, H. F. Hamann, and S. J. McNab, *Nature (London)* **438**, 65 (2005).
- <sup>2</sup>L. Gu, W. Jiang, X. Chen, and R. T. Chen, *IEEE J. Sel. Top. Quantum Electron.* **14**, 1132 (2008).
- <sup>3</sup>J. H. Wülber, S. Prorok, J. Hampe, A. Petrov, M. Eich, J. Luo, A. K.-Y. Jen, M. Jenett, and A. Jacob, *Opt. Lett.* **35**, 2753 (2010).
- <sup>4</sup>Y. A. Vlasov and S. J. McNab, *Opt. Lett.* **31**, 50 (2006).
- <sup>5</sup>Y. Cui, K. Liu, D. L. MacFarlane, and J.-B. Lee, *Opt. Lett.* **35**, 3613 (2010).
- <sup>6</sup>N. Ozaki, Y. Kitagawa, Y. Takata, N. Ikeda, Y. Watanabe, A. Mizutani, Y. Sugimoto, and K. Asakawa, *Opt. Express* **15**, 7974 (2007).
- <sup>7</sup>S. G. Johnson, P. Bientman, M. A. Skorobogatiy, M. Ibanescu, E. Lidorikis, and J. D. Joannopoulos, *Phys. Rev. E* **66**, 066608 (2002).
- <sup>8</sup>P. Pottier, M. Gnan, and R. M. De La Rue, *Opt. Express* **15**, 6569 (2007).
- <sup>9</sup>C.-Y. Lin, X. Wang, S. Chakravarty, B. S. Lee, W.-C. Lai, and R. T. Chen, *Appl. Phys. Lett.* **97**, 183302 (2010).
- <sup>10</sup>J. P. Hugonin, P. Lalanne, T. P. White, and T. F. Krauss, *Opt. Lett.* **32**, 2638 (2007).
- <sup>11</sup>C. Martijn de Sterke, K. B. Dossou, T. P. White, L. C. Botten, and R. C. McPhedran, *Opt. Express* **17**, 17338 (2009).
- <sup>12</sup>S. Hughes, L. Ramunno, J. F. Young, and J. E. Sipe, *Phys. Rev. Lett.* **94**, 033903 (2005).
- <sup>13</sup>R. J. P. Engelen, D. Mori, T. Baba, and L. Kuipers, *Phys. Rev. Lett.* **101**, 103901 (2008).
- <sup>14</sup>M. Patterson, S. Hughes, S. Combrié, N. V. Tran, A. De Rossi, R. Gabet, and Y. Jaouën, *Phys. Rev. Lett.* **102**, 253903 (2009).
- <sup>15</sup>A. Alù, M. G. Silveirinha, and N. Engheta, *Phys. Rev. E* **78**, 016604 (2008).